VSV strains with defects in their ability to shutdown innate immunity are potent systemic anti-cancer agents

David F. Stojdl,[1] Brian D. Lichty,[1] Benjamin R. tenOever,[2] Jennifer M. Paterson,[1,6] Anthony T. Power,[1,6] Shane Knowles,[1] Ricardo Marius,[1] Jennifer Reynard,[1] Laurent Poliquin,[3] Harold Atkins,[1] Earl G. Brown,[6] Russell K. Durbin,[4] Joan E. Durbin,[4] John Hiscott,[2,5] and John C. Bell[1,6,*]

[1]Ottawa Regional Cancer Centre Research Laboratories, 501 Smyth Road, Ottawa, Ontario, Canada K1H 8L6.
[2]Terry Fox Molecular Oncology Group, Lady Davis Institute for Medical Research, McGill University, Montreal, Quebec, Canada
[3]Department of Biological Sciences, Université du Québec à Montréal, P.O. Box 8888, Station Centre-ville, Quebec, H3C 3P8, Montreal, Canada
[4]Children's Research Institute, Children's Hospital, Columbus, Department of Pediatrics, College of Medicine and Public Health, The Ohio State University, Columbus, Ohio 43205
[5]Departments of Microbiology and Immunobiology, Medicine, McGill University, Montreal, Quebec, Canada H3T 1E2
[6]Department of Biochemistry, Microbiology and Immunology, University of Ottawa, 451 Smyth Road, Ottawa, Ontario, Canada K1H 8M5
*Correspondence: John.bell@orcc.on.ca

Summary

Ideally, an oncolytic virus will replicate preferentially in malignant cells, have the ability to treat disseminated metastases, and ultimately be cleared by the patient. Here we present evidence that the attenuated vesicular stomatitis strains, AV1 and AV2, embody all of these traits. We uncover the mechanism by which these mutants are selectively attenuated in interferon-responsive cells while remaining highly lytic in 80% of human tumor cell lines tested. AV1 and AV2 were tested in a xenograft model of human ovarian cancer and in an immune competent mouse model of metastatic colon cancer. While highly attenuated for growth in normal mice, both AV1 and AV2 effected complete and durable cures in the majority of treated animals when delivered systemically.

Introduction

Over the last decade, a variety of replicating oncolytic viruses have been selected or engineered to be therapeutics that exploit genetic defects unique to tumor cells (reviewed in Bell et al., 2002; Gromeier and Wimmer, 2001; Hawkins et al., 2002; Kruyt and Curiel, 2002; Norman et al., 2000)). One genetic defect frequently arising during tumor evolution, is diminished interferon (IFN) responsiveness (Bello et al., 1994; Linge et al., 1995; Lu et al., 2000; Matin et al., 2001; Sun et al., 1998; Wong et al., 1997). This reflects the important role that interferon-regulated pathways play in the control of normal cell growth and apoptosis. Interferon is also a key mediator of the individual cell's antiviral response and thus tumor cells, which acquire mutations allowing them to escape interferon-mediated growth control programs, will simultaneously compromise their innate antiviral response. We hypothesized that viruses whose replication is inhibited by interferon should grow well in tumor but not normal cells. We and others have found that vesicular stomatitis virus (VSV), whose growth is strongly inhibited by interferon, is a potent oncolytic virus (Balachandran and Barber, 2000; Stojdl et al., 2000b). In fact, while VSV infections are uniformly fatal to nude mice (Huneycutt et al., 1993; Stojdl et al., 2000b), we found that prophylactic interferon treatment can rescue even immunocompromised animals while preserving virus-mediated oncolysis. We reasoned that a virus that both induces the production of interferon and is susceptible to its antiviral affects would be a superior therapeutic. Here we describe two naturally occurring VSV variants that possess both these properties. The VSV variants retain oncolytic activity in vitro and in a variety of in vivo models but because of their potent induction of interferon have a vastly improved therapeutic index over their wild-type (WT) counterpart.

Results

Attenuation of VSV in vivo is dependent upon intact interferon signaling pathways

Two variants of VSV that produce small plaques on interferon-responsive cells (herein referred to as AV1 and AV2) were found

SIGNIFICANCE

A key limitation to the application of viruses as cancer therapeutics is the possibility of uncontrolled virus growth in normal tissues, potentially leading to treatment complications or disease. Here, we describe novel, oncolytic variants of vesicular stomatitis virus (VSV) that not only have potent anti-tumor activity in vivo, but establish an anti-viral state that protects against the toxicity associated with infection of healthy cells. Our work has uncovered the mechanism that virulent VSV strains use to defeat host antiviral defences, furthering our understanding of early IFN signaling in response to a viral invader. These findings have directed us toward the development of improved VSV-based oncolytic viruses and are generally applicable to a wide range of viral based therapeutics.

A

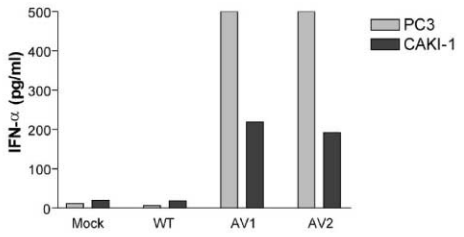

B

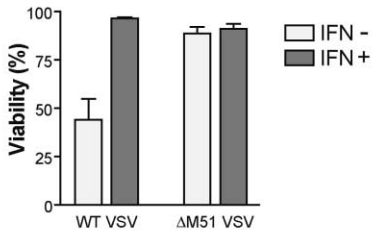

C

	LD50 (pfu)		
	WT	**AV1**	**AV2**
IN			
Balb/c	$1x10^4$	$3 x10^8$	$2.5 x10^8$
CD-1	$1 x10^6$	$2x10^8$	nd
IV			
CD-1	$1x10^8$	$8 x10^9$	nd

D

	Serum IFN (pg/ml)		
Time (h)	*Naïve (n=2)*	*WT (n=3)*	*AV3 (n=3)*
0	neg.	neg.	neg.
1	neg.	neg.	559 +/- 116
6	neg.	8197 +/- 2726	25213 +/- 322

neg. = below the level of detection of the assay (<200 pg/ml); time refers to hours post infection

E

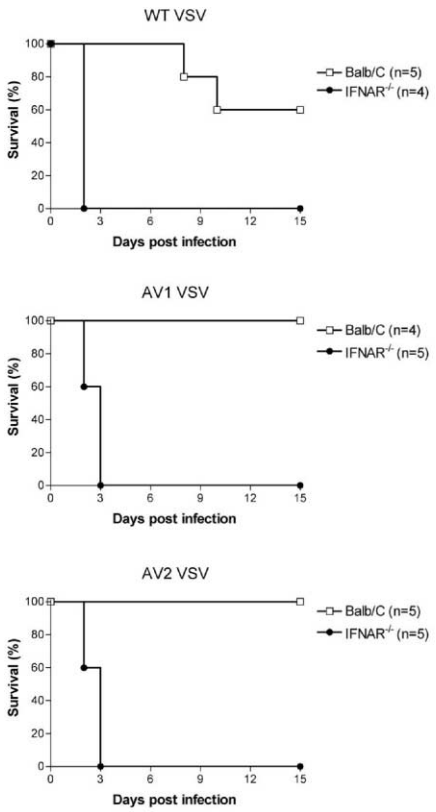

F

	PFU	Morbidity	Mortality
WT VSV	10^1	3/3	3/3
AV2	10^7	0/3	0/3
AV2 (10^6) + WT VSV	10^1	0/3	0/3
	10^2	0/3	0/3
	10^3	0/3	0/3

Figure 1. Decreased in vivo toxicity of AV1 and AV2 is mediated by interferon

A: Human prostate carcinoma cells (PC3) and human renal carcinomas cells (CAKI-1) were either mock infected or infected with wild-type (WT), AV1, or AV2 strains of VSV. Culture media were assayed by ELISA to detect human IFN-α production 48 hr post-infection.

B: Exogenous interferon is required to protect MEFs from WT GFP but not from AV3 GFP. Balb/C MEFs were pretreated with 0 or 30 U/ml universal type I interferon for 16 hr and then infected with WT GFP VSV or AV3 GFP at an MOI of 0.1. Twenty-four hours later, cell viability was measured by MTS assay.

C: In vivo toxicity of WT versus mutant VSV strains by route and mouse strain. IN = intranasal; IV = intravenous; nd = not determined.

D: AV3 induces IFN-α quicker and to a greater degree than WT VSV in vivo. Groups of mice were either mock infected or infected with WT GFP or AV3 GFP, and their serum IFN-α levels were assayed at the indicated times post-infection.

E: Balb/C and Balb/C *INFAR*$^{-/-}$ mice were infected intranasally with WT VSV, AV1, or AV2 virus and monitored for morbidity.

F: AV2 can protect mice against lethal WT VSV infection. *PKR*$^{-/-}$ mice were infected intranasally at various doses with either WT, AV2, or both and monitored for morbidity or mortality. Values denote number of mice per group.

to induce from twenty to fifty times more interferon α (IFN-α) than WT VSV following infection of epithelial cell lines (Figure 1A). Sequencing of the variants revealed that they differed from the wild-type strain in their M proteins with a single amino acid substitution in the case of AV1 (M51R) and two amino acids (V221F and S226R) in AV2. A third variant was created to be a mimetic of AV1 by complete deletion of methionine 51 (MΔ51 or AV3) and found to have biological properties indistinguishable from AV1 and AV2. As expected (Stojdl et al., 2000b), primary mouse embryo fibroblasts are protected against WT VSV infection only in the presence of exogenously added interferon whereas MEFs (mouse embryonic fibroblasts) are refractory to infection by the interferon inducing mutant AV3 (Figure 1B).

In animals, the role of the interferons in protecting against virus infection and the mechanisms underlying their induction are more complex than in the simple tissue culture systems described above (Barchet et al., 2002; Levy, 2002). Nevertheless, we show in the following that the AV strains are more potent interferon inducers and have reduced toxicity in mice in a strictly interferon-dependent fashion. For example, mice

infected intravenously can tolerate some 80 times more AV1 virus than WT VSV, and AV3 induced a more rapid and robust production of interferon than WT VSV (Figures 1C and 1D). The critical role that interferon signaling plays in the protection of mice from infection by AV1 and AV2 was verified using interferon receptor knockout (*INFAR*$^{-/-}$) animals. The LD_{50} of AV1 and AV2 when delivered intranasally to Balb/C (*INFAR*$^{+/+}$) mice was determined to be 10,000 times greater than WT VSV delivered by the same route (Figure 1C). Similar results were seen in CD-1 mice (WT $= 1 \times 10^6$; AV1 $= 2 \times 10^8$ pfu). However, in the absence of a functional interferon receptor, AV1 and AV2 were as toxic as wild-type virus, indicating that the attenuation of AV1 and AV2 growth in vivo is dependent upon an intact interferon system (Figure 1E).

The AV1 and AV2 variants protect mice from infection by WT VSV

Mice that lack the double-stranded RNA-dependent kinase (PKR) gene are known to be exquisitely sensitive to infection by wild-type vesicular stomatitis virus, although PKR$^{-/-}$ fibroblasts can be protected by prophylactic treatment with interferon (Balachandran et al., 2000). Since AV1 and AV2 strongly induce interferon production during the course of a natural infection, we tested whether PKR$^{-/-}$ mice would be resistant to infection by these viruses. Indeed we found that while $<$10 pfu of wild-type VSV can kill PKR$^{-/-}$ mice (Figure 1F), doses greater than 10^7 pfu of AV1 and AV2 were well tolerated by PKR$^{-/-}$ animals. More strikingly, when coinfected with AV2, the LD_{100} of wild-type VSV was dramatically increased in PKR$^{-/-}$ animals. Indeed, doses 100 times greater than the LD_{100} for WT VSV were well tolerated when coinfected with AV2 (Figure 1F). Given that PKR$^{-/-}$ fibroblasts can be protected from WT VSV infection by prophylactic interferon administration (Balachandran et al., 2000), that the AV variants induce interferon, and that AV variants are toxic in mice that lack a functional interferon receptor, we believe that the protective effect of AV2 on PKR$^{-/-}$ mice is most easily explained by the ability of these viruses to strongly induce interferon production in the infected animal.

Wild-type, AV1 and AV2 viruses trigger antiviral responses in infected cells

We used microarray and Western blot analysis over a time-course of virus infection to allow us to detect early signaling events triggered by WT and AV variants that lead to the transcriptional activation of antiviral genes. Others have established that an early response to virus infection is the phosphorylation and activation of the latent transcription factor IRF-3 (Sato et al., 1998b). It appears that WT, AV1 and AV2 viruses trigger IRF-3 phosphorylation with similar kinetics (Figure 2A). Following phosphorylation, IRF-3 assembles together with CBP/300 and, along with other transcription factors (e.g., NFκB and c-JUN/ATF-2), initiates the transcription of a number of antiviral gene products (Wathelet et al., 1998). As shown in Table 1, microarray analysis revealed that a large number of genes were dramatically induced 3 hr post-infection with all three viruses. Many of these genes are known to be activated by virus infection (Nakaya et al., 2001), including several that are directly regulated following activation of the latent transcription factors IRF-3, NFκB, and c-JUN/ATF-2 (Genin et al., 2000). We validated the microarray data by performing RT-PCR analysis on a sampling of gene products (Figure 2B).

In Figures 2C–2E, we present a model in which virus infection leads to waves of transcriptional events that are sequential and interdependent. For example, genes that we refer to herein as primary response genes were induced 3–6 hr post-infection by all three viruses (Figures 2B and 2C). On the other hand, secondary response genes that require the production of IFN-β protein and the autocrine activation of the JAK/STAT pathway (Figure 2D) were differentially induced by the wild-type and attenuated viruses (see IRF-7 in Figures 2A and 2D). As a consequence of the impaired IRF-7 production in WT VSV-infected cells, tertiary response gene products like the IFN-α transcripts were not induced in wild-type VSV-infected cells (Figure 2E). These results indicate that all three viruses *trigger* activation of IRF-3 and the subsequent transcription of a cohort of genes that we call primary response genes. We hypothesized that the M protein encoded by wild-type VSV *disables* the host cell's antiviral response by disrupting subsequent activation of secondary and tertiary response genes.

VSV M protein blocks the nuclear export of interferon-β mRNA

It has been suggested that VSV M protein either blocks the transcription of the *IFN*-β gene (Ahmed et al., 2003; Ferran and Lucas_Lenard, 1997), inhibits the nuclear export of mRNAs (Her et al., 1997; von Kobbe et al., 2000), or interferes with JAK/STAT signaling (Terstegen et al., 2001). Our transcript profiling studies would be consistent with either of the latter two mechanisms; however, we have been unable to show any impairment in the induction of the JAK/STAT pathway by exogenous interferon in infected cells (data not shown). On the other hand, when we used microarray or RT-PCR analysis to compare and contrast transcripts in nuclear and cytoplasmic fractions, we found clear differences between wild-type and attenuated virus-infected cells (Figure 3A). Importantly, *IFN*-β mRNA although induced in nuclear fractions by all three viruses was not found in the cytoplasmic pool of mRNAs in WT infected cells. Furthermore, IFN-β was undetectable in culture media from cells infected with WT VSV, while copious amounts of the cytokine were produced from cells infected with either AV1 or AV2 (Figure 3B). Two additional experiments help shed light upon how WT VSV subverts the interferon signaling pathway. First, cells were infected with either WT or AV3 VSV, and at 22 hr post-infection, IFN-α production in tissue culture supernatant was measured. WT VSV does not induce the production of IFN-α while AV3 is a potent inducer (Figure 3C). The induction of IFN-α by AV3 was dependent upon prior production of IFN-β as inclusion of neutralizing anti-IFN-β antibody to infected cultures inhibited IFN-α production from these cells (Figure 3C). Second, we constructed a wild-type VSV that expresses a constitutively active version of IRF-7. This virus has an attenuated phenotype and induces the expression of *IFN*-α genes within 4 hr post-infection, even in the presence of wild-type VSV M protein (Figure 2D). In total, these results are consistent with the idea that wild-type VSV triggers a primary antiviral response, but through coordinate expression of viral gene products blunts secondary and tertiary responses by blocking nuclear export of critical antiviral mRNAs.

AV1 and AV2 retain their ability to kill tumor cells in vitro and in vivo

To assess the oncolytic properties of the attenuated VSV strains, the NCI human tumor cell panel (60 cell lines from a spectrum

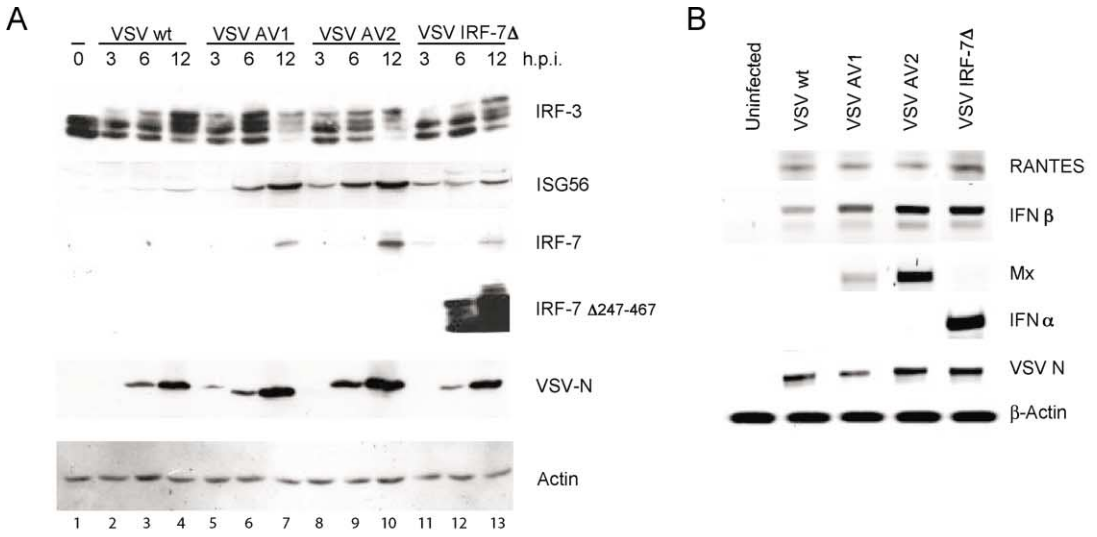

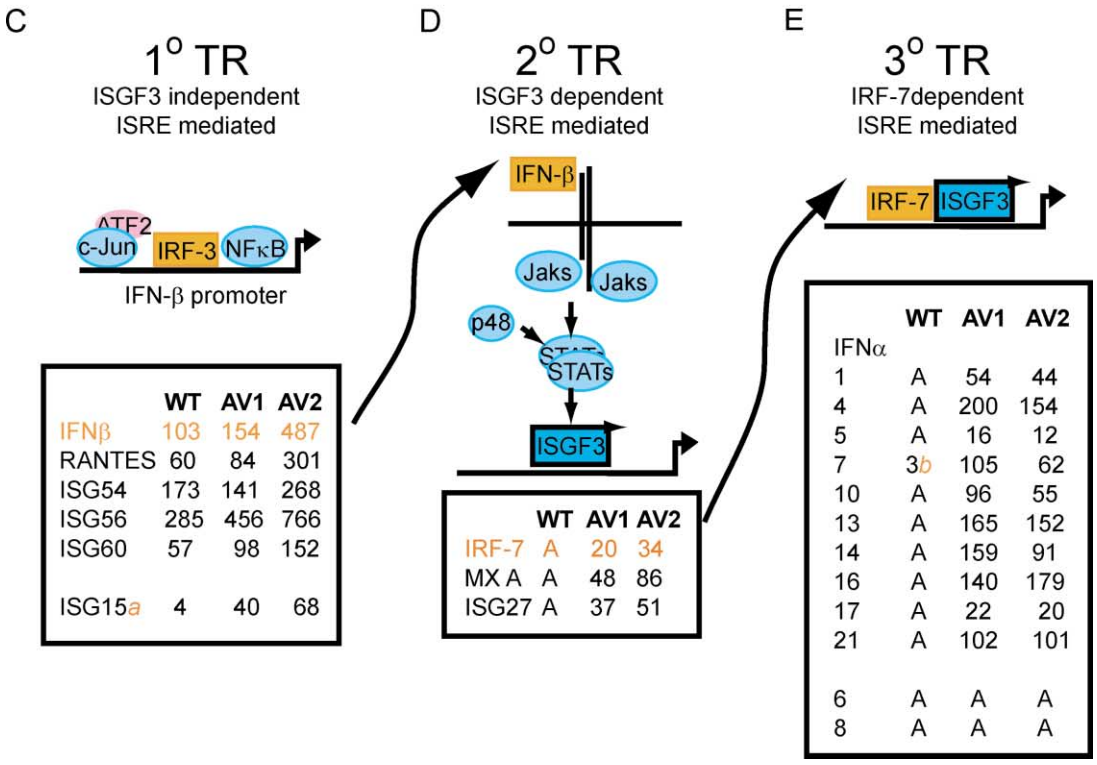

	WT	AV1	AV2
IFNβ	103	154	487
RANTES	60	84	301
ISG54	173	141	268
ISG56	285	456	766
ISG60	57	98	152
ISG15*a*	4	40	68

	WT	AV1	AV2
IRF-7	A	20	34
MX A	A	48	86
ISG27	A	37	51

IFNα	WT	AV1	AV2
1	A	54	44
4	A	200	154
5	A	16	12
7	3*b*	105	62
10	A	96	55
13	A	165	152
14	A	159	91
16	A	140	179
17	A	22	20
21	A	102	101
6	A	A	A
8	A	A	A

Figure 2. The secondary transcriptional response is inhibited by WT VSV but not AV1 or AV2

A: Western blot analysis showed similar kinetics of IRF-3 activation between WT and mutant VSVs; however, ISG56 (primary response) protein expression was severely impaired in WT infected cells. IRF-7 protein is detected only in AV1- and AV2-infected cells. IRF-7Δ appears to be able to induce the expression of endogenous IRF-7.

B: RT-PCR data at 4 hr post-infection of A549 cells showed primary response genes *RANTES* and *IFN*-β induced to similar levels in WT and mutant VSV-infected cells while upregulation of *MX1* (secondary response) was impaired in WT infected cells.

C: Primary response to viral infection is mediated by IRF-3, cJUN/ATF-2, and NFκB (shown here forming part of the enhancesome complex at the *IFN*-β promoter). Microarrray data indicate primary transcriptional response genes robustly upregulated in both WT and mutant virus-infected cells. (*a*: *ISG15* is known to require ISGF3 for full induction). Values represent fold induction over mock infected.

D: *IFN*-β is then translated and secreted to stimulate, in an autocrine fashion, JAK/STAT signaling to form ISGF3 complexes in the nucleus, which mediates the induction of genes of the secondary transcriptional response. While cells infected with AV1 or AV2 show robust upregulation of these genes, WT infected cells show no expression at all (A = absent).

E: Without the consequent expression of IRF-7 in cells infected with WT VSV, the tertiary transcriptional wave, which includes almost all *IFN*-α genes, cannot take place (*b*: *IFN*-α*7* is marginally detected by the array in WT samples). In contrast, AV1- and AV2-infected cells efficiently induce the expression of *IFN*-α genes.

Table 1. Microarray analysis of the transcriptional response to VSV infection over time

		WT			AV1			AV2		
		Hours post infection			Hours post infection			Hours post infection		
Accession #	Common name	3	6	12	3	6	12	3	6	12
Primary transcriptional response										
NM 000201.1	CD54	2.3	A	A	3.3	3.0	33.6	2.7	5.4	56.8
NM 016323.1	CEB1	2.0	21.2	204.4	1.6	38.0	279.3	1.9	73.6	490.5
U83981	GADD34	10.8	57.5	95.0	3.1	48.8	422.7	5.5	159.0	686.7
NM_002176.1	**IFN beta**	**4.2**	**103.2**	**488.6**	**3.2**	**154.5**	**1531.6**	**3.6**	**487.3**	**2157.9**
NM 000600.1	IL6	7.3	19.1	38.2	3.8	44.7	171.6	7.4	120.3	238.7
BE888744	ISG54	19.5	173.1	804.5	4.7	141.0	721.9	11.4	268.4	1357.8
NM_00 1548.1	ISG56	32.3	285.9	855.2	20.0	456.8	1411.7	39.8	766.0	1992.1
NM_00 1549.1	ISG60	7.6	57.5	238.0	4.1	97.7	288.6	7.0	151.6	457.7
AF063612.1	OASL	6.6	71.8	222.0	3.4	81.9	388.9	5.7	172.0	776.9
NM_021127.1	PMAIP1	5.2	22.1	58.6	2.1	17.3	87.5	4.3	34.3	169.8
NM_002852.1	PTX3	5.9	3.1	A	6.4	11.7	114.0	4.9	29.9	117.6
AF332558.1	PUMA	10.6	A	A	A	38.7	211.6	9.8	77.8	428.0
NM 002985.1	RANTES	3.4	60.1	945.0	2.6	84.9	1796.7	4.1	301.8	3916.1
AY029 180.1	SUPAR	3.7	9.8	14.7	2.4	10.5	40.5	2.8	27.7	46.3
NM_006290.1	TNFAIP3	2.8	6.3	15.5	2.7	13.8	83.5	3.1	30.5	152.8
Secondary transcriptional response										
NM_030641.1	APOL6	A	A	A	A	15.3	40.8	A	25.2	37.3
AF323540.1	APOLL	1.8	A	A	1.0	11.3	25.7	2.2	10.7	34.5
U84487	CX3C chemokine precursor	2.0	2.5	2.5	1.7	7.0	45.1	2.3	14.1	65.9
BC002666.1	GBP1	A	A	4.2	A	35.9	171.6	1.4	66.2	249.2
NM_006018.1	HM74	A	A	A	2.2	29.1	72.5	A	66.4	45.4
NM_031212.1	hMRS3/4	A	A	A	2.5	4.2	21.3	A	10.1	18.3
NM 005531.1	IFI16	A	A	A	2.4	12.8	38.1	2.8	18.9	46.2
NM_005532.1	IFI27	A	A	21.9	A	36.6	281.0	A	51.0	295.4
NM 004509.1	IFI41	A	A	A	A	10.0	22.8	1.3	11.9	18.1
NM_022873.1	IFI-6-16	0.9	2.5	2.2	0.7	7.0	15.6	1.1	9.6	15.7
NM_003641.1	IFITM1	1.9	A	A	1.2	8.5	67.1	1.9	14.3	42.1
AA749101	IFITM1	1.2	3.1	2.3	1.0	6.6	40.9	1.2	9.5	32.6
NM 000882.1	IL12A	1.6	A	A	A	4.9	13.7	A	6.5	28.8
M15329.1	IL1A	nd	A	A	A	8.3	79.4	A	27.0	287.6
NM_004030.1	**IRF7**	**1.4**	**A**	**A**	**A**	**19.9**	**109.9**	**2.2**	**33.7**	**144.3**
NM_006084.1	IRF9	A	A	1.2	1.6	6.5	11.2	1.5	7.8	17.4
BC001356.1	ISG35	1.1	A	A	1.0	5.8	23.2	1.4	7.1	20.2
AF280094.1	ISG75	1.3	1.8	2.2	1.5	10.3	16.2	1.2	12.5	13.8
AF280094.1	ISG75	0.9	1.7	A	1.2	7.5	10.8	1.5	9.5	11.1
U 17496.1	LMP7	A	A	A	A	7.6	15.3	0.9	10.0	10.4
NM_006417.1	MTAP44	A	A	23.3	A	10.8	82.7	A	18.0	133.9
NM_002462.1	MX A	A	A	27.6	A	48.1	261.9	A	85.7	232.9
AB014515	NEDD4 BP1	A	A	9.2	2.0	4.0	13.1	1.5	4.5	19.5
NM_002759.1	PKR	0.5	0.9	2.0	0.8	4.3	15.2	1.0	6.6	9.6
NM_021 105.1	PLSCR1	1.4	1.7	A	2.2	5.0	24.9	2.1	4.9	15.1
NM_017912.1	putative Ub ligase	A	A	19.1	A	9.6	26.3	A	12.5	24.8
BF939675	SECTM1	A	A	A	A	20.7	93.8	A	24.8	33.9
BC004395.1	Similar to apolipoprotein L	A	A	A	A	11.7	17.2	A	14.6	21.3
NM_003141.1	SSA1	A	A	A	1.2	5.9	11.2	1.4	7.9	11.1
AA083478	STAF50	nd	A	nd	1.7	8.5	96.3	nd	16.7	56.1
NM_005419.1	STAT2	1.1	A	A	1.3	3.0	9.1	1.1	4.3	9.1
NM_003810.1	TRAIL	A	A	A	A	22.4	135.4	0.7	37.3	88.6
NM_020119.1	ZAP	A	A	19.4	0.9	4.6	79.9	A	11.4	133.8
Tertiary transcriptional response										
M 12350.1	IFN-27	A	A	A	nd	nd	102.3	nd	A	101.4
NM_024013.1	**IFNA1**	**nd**	**A**	**A**	**nd**	**2.2**	**53.6**	**nd**	**A**	**44.0**
NM_002171.1	IFNA10	A	A	A	A	A	96.2	A	A	55.1
NM_006900.2	IFNA13	A	A	A	A	A	165.4	nd	A	152.1
NM_002 172.1	IFNA14	A	A	A	A	A	159.0	A	4.4	91.1
NM_002 173.1	IFNA16	1.0	A	1.8	1.1	0.9	139.9	0.7	3.3	95.7
M38289.1	IFNA17	A	A	A	A	A	21.5	A	A	19.8
NM_002 169.1	IFNA5	1.0	A	A	0.9	A	16.4	0.9	A	11.6
NM_021057.1	IFNA7	A	A	3.5	A	A	105.0	A	3.4	61.7

Data represented as fold change compared to mock-infected samples. All samples are from nuclear fractions of infected cells.
A = Absent (no detectable mRNA); nd = no data; bold genes represent "archetypal genes," see text for explanation.

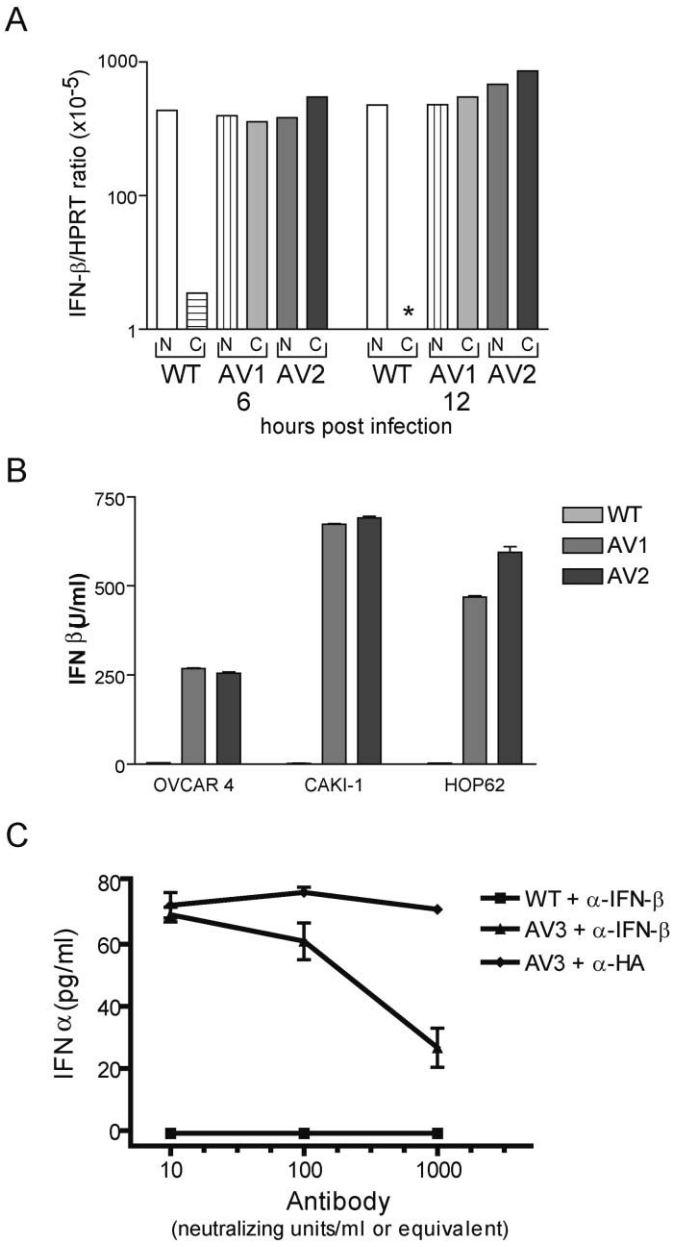

Figure 3. WT VSV inhibits IFN-β mRNA nuclear/cytoplasmic transport and blocks IFN-α production

A: *IFN*-β mRNAs are severely depleted in cytoplasmic fractions from WT VSV-infected cells as determined by quantitative RT-PCR. Nuclear (N) and cytoplasmic (C) total RNA fractions from cells infected with WT, AV1, or AV2 VSV were assayed for *IFN*-β mRNA, normalized to *HPRT* mRNA from the same sample. * indicates no *IFN*-β mRNA detected.

B: Cells infected with either WT or mutant VSV strains were assayed by ELISA for IFN-β production. AV1- and AV2-infected cells and not WT VSV-infected cells produce secreted IFN-β.

C: Blocking IFN-β inhibits the production of IFN-α. OVCAR-4 cells were infected with mutant VSV in the presence of neutralizing antibody to IFN-β or an irrelevant antibody and subsequently assayed by ELISA for IFN-α production.

of malignancies) was challenged with either WT, AV1, or AV2 viruses and assayed for metabolic cell death 48 hr later. It is clear from Table 2A that WT VSV is able to infect and kill a wide range of cancer cell types, and furthermore, the majority of cancer cell lines tested demonstrated impaired responses to either IFN-α or IFN-β (Table 2B). AV1 and AV2 were as effective at killing these interferon nonresponsive tumor cell lines as WT VSV.

We previously reported the successful treatment of subcutaneous xenograft tumors in nude mice with WT VSV; however, in these experiments, exogenous interferon was required to protect the animals from succumbing to viral infection. Our results with the NCI cell panel suggest that AV1 and AV2 should efficiently kill tumor cells with little toxicity in mouse models even in the absence of interferon treatment, and therefore we conducted an extensive analysis of the in vivo oncolytic properties of the AV variants. In a first series of experiments, human ovarian carcinoma cells were injected into the peritoneal cavity of CD-1 nude mice and allowed to grow for 12 days. Mice (14/15) receiving UV-inactivated virus developed ascites by day 15 post-treatment. In contrast, three doses of AV2 delivered into the peritoneal cavity provided durable cures in 70% of the mice (Figure 4A). Remarkably, while a single therapeutic dose of WT VSV is uniformly lethal to nude mice (Stojdl et al., 2000b), none of the animals treated with three doses of AV2 exhibited even symptoms of virus infection.

Systemic treatment in immune-competent mouse models

Earlier preclinical, clinical, and mathematical modeling studies (Wein et al., 2003) predict that greatest anti-tumor efficacy is achieved when the delivered virus is distributed diffusely throughout the tumor (e.g., through tumor vasculature). Given that certain oncolytic viruses are rapidly inactivated in blood or inhibited by physical barriers (Ikeda et al., 2000; Wakimoto et al., 2002, 2003; Yoon et al., 2001), we felt it was important to determine the minimum VSV doses required to achieve effective delivery of VSV into tumor sites. For these studies, we engineered a VSV strain to express GFP during productive infections and examined subcutaneous tumors 24 hr after intravenous virus administration. Virus doses in the range of 10^8–10^9 pfu per mouse gave optimum tumor delivery (Figure 5). In other experiments and those shown below, we found that virus administered in this dose range also provided maximum therapeutic benefit to tumor-bearing animals. For example, subcutaneous tumors were established by injecting CT26 colon carcinoma cells into the hind flank of syngeneic Balb/c mice. Once tumors became palpable (approximately 10 mm^3), virus was administered via tail vein injection. Twelve days post-treatment, mice receiving UV-inactivated VSV reached endpoint with an average tumor size of 750 mm^3. In contrast, a single treatment with AV2 showed significant efficacy, delaying the time to endpoint by almost 3-fold (34 days). Of the eight animals in this treatment group, seven were considered partial responders while only one mouse did not respond to the treatment (data not shown). When multiple doses of AV1 or AV2 were given intravenously, the efficacy of the treatments was markedly increased (Figure 4B). With the exception of one animal, all tumors responded to treatment with AV1, with 3/6 mice showing complete tumor regression. Two of these mice showed complete regressions as early as day 8 and 9, respectively, post-infection. Two of the re-

Table 2A. Mutant VSV strains are highly lytic on members of the NCI 60 panel of cancer cell lines

	WT		AV1		AV2	
		MOI		MOI		MOI
Leukemia	67% (4/6)*	0.13	nd		60% (3/5)	0.02
NSC lung carcinoma	78% (7/9)	0.02	60% (3/5)	0.001	75% (6/8)	0.19
Colon carcinoma	86% (6/7)	0.037	100% (5/5)	0.001	100% (6/6)	0.017
CNS	80% (4/5)	0.02	50% (1/2)	0.6	60% (3/5)	0.38
Melanoma	75% (6/8)	0.1	100% (2/2)	0.15	63% (5/8)	0.25
Ovarian carcinoma	100% (6/6)	0.3	67% (2/3)	0.0005	60% (3/5)	0.14
Renal carcinoma	88% (7/8)	0.24	100% (3/3)	0.14	100% (7/7)	0.48
Prostate	100% (2/2)	0.06	100% (2/2)	0.035	100% (2/2)	0.04
Breast	83% (5/6)	0.009	75% (3/4)	0.005	60% (3/5)	0.12
All cell lines tested	82% (47/57)	0.11	80% (21/26)	0.07	75% (38/51)	0.20

*Percent of NCI 60 panel cell lines by tumor type deemed highly sensitive to virus infection. () denote the number of highly susceptible cell lines out of the number of cell lines tested. Cell line deemed highly susceptible if the $EC_{50} \leq$ MOI of 1 following a 48 hr infection. *MOI* represents average EC_{50} (MOI) of susceptible cell lines. nd = not determined.

maining animals showed partial responses, delaying tumor progression by almost 2-fold compared to controls. All eight AV2-infected mice responded well to treatment with five of eight developing durable tumor regressions. In fact, no sign of tumor regrowth was evident even 7 months post-treatment. Furthermore, these mice failed to produce tumors when rechallenged with CT26 cells 7 months post-treatment, with no trace of detectable virus, perhaps indicating that host-mediated immunity to the tumor had developed. All forms of intravenous treatment were well tolerated by the mice, with no mortalities occurring and minimal signs of morbidity. Infected mice had mild to medium piloerection, mild dehydration, and some transient body weight loss following the initial treatment (Figure 4C). These symptoms were only observed after the initial infection, and all subsequent doses failed to elicit any signs of infection.

Systemic administration of AV1 and AV2 is effective against disseminated disease

CT-26 cells, when injected into the tail vein, seed tumors throughout the mouse, although predominantly within the lungs. We examined the lungs of four mice 16 days after tumor cell injection and four days after treatment with UV-inactivated virus (Figure 4D). These lungs were three times their normal mass due to their tumor burden. In contrast, tumor-bearing littermates receiving a single intravenous or intranasal dose of AV2 4 days prior to the time of sacrifice had lungs with normal mass and few obvious tumor nodules (Figure 4D). Consistent with this result, viral gene expression could be detected within 24 hr of a single intravenous dose of GFP-expressing AV3 in all tumor nodules, with little or no detectable expression in normal lung tissue (Figure 4D; inset).

Figure 4E shows the survival plots of mice seeded with lung tumors and then treated intranasally with UV-inactivated virus, AV1 or AV2. The mean time to death (MTD) of animals treated with UV-inactivated virus was approximately 20 days. However, mice treated with either AV1 or AV2 were completely protected. This experiment demonstrates the remarkable ability of AV1 and AV2 to produce durable cures in an aggressive, disseminated, immune-competent tumor model.

Table 2B. The majority of cell lines in the NCI 60 cell panel show IFN defects

	Type I IFN defects
Leukemia	100% (6/6)*
NSC Lung carcinoma	71% (5/7)
Colon carcinoma	100% (7/7)
CNS	75% (3/4)
Melanoma	85% (6/7)
Ovarian carcinoma	67% (4/6)
Renal carcinoma	75% (6/8)
Prostate	100% (2/2)
Breast	60% (3/5)
All cell lines tested	81% (42/52)

*Denotes the number of cells in each group, which were unresponsive to either IFN-α or IFN-β pre-treatment. Cell line deem unresponsive if IFN pre-treatment was unable to significantly affect (<10-fold) the EC50 of cells infected with WT VSV for 48 hr.

Discussion

A key difference between the attenuated viruses described here and previously reported oncolytic versions of VSV is the inability of mutant M proteins of the AV viruses to block interferon production in infected cells. VSV M is a multifunctional protein required for several key viral functions including budding (Jayakar et al., 2000), virion assembly (Newcomb et al., 1982), cytopathic effect (Blondel et al., 1990), and inhibition of host gene expression (Lyles et al., 1996). The latter property has been attributed to the ability of M to block host RNA polymerase activity (Ahmed et al., 2003; Yuan et al., 2001) or to inhibit the nuclear transport of both proteins and mRNAs into and out of the host nucleus (Her et al., 1997; von Kobbe et al., 2000). The results presented here using virus infection are consistent with blocks in nuclear transport being the major mechanism by which wild-type VSV strains mitigate host antiviral response. Our analysis of infected cell transcripts provided little evidence to support a role for M protein in inhibiting host cell transcription but rather shows that VSV infection triggers an IRF-3-mediated stimulation of antiviral genes followed by an M protein-mediated block of transport of primary response transcripts from infected cell nuclei. Particularly germane to this study is the work from Dahlberg's group (Petersen et al., 2000) and others (von Kobbe et al., 2000) that has shown, by transfection studies, that M protein can associate with nuclear pore proteins and effect a block in mRNA export possibly through an association with the

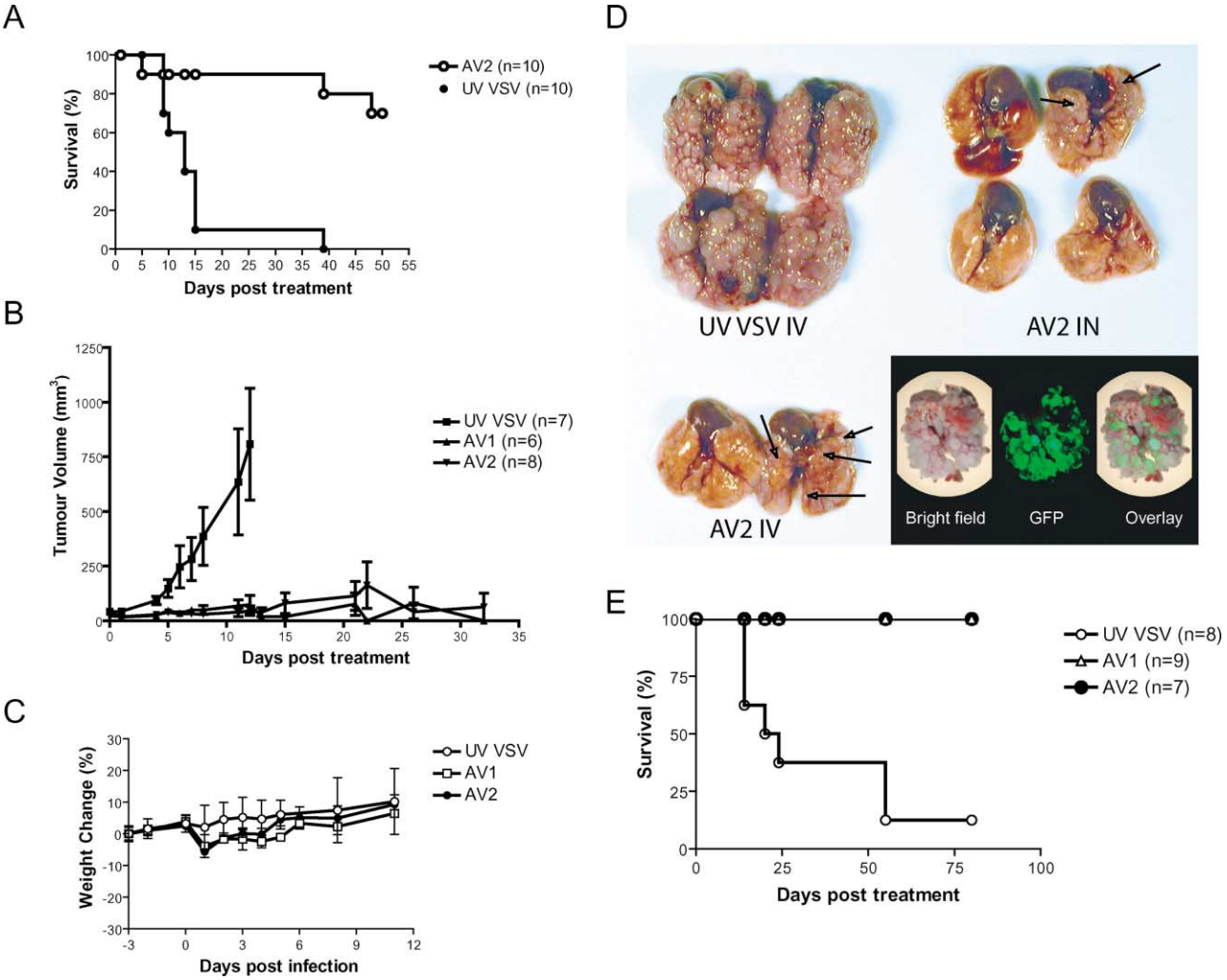

Figure 4. AV strains are efficacious in mouse tumor models

A: AV2 is effective in treating human ovarian tumor xenografts. 1×10^6 human ES-2 ovarian carcinoma cells were injected into the intraperitoneal cavity of CD-1 nude mice. Twelve days later, animals were treated by intraperitoneal injection every other day with either AV2 or UV-inactivated AV2 (1×10^9 pfu/dose; three doses total). Animals were assessed for morbidity and mortality and euthanized following the appearance of moderate ascites formation. "*n*" denotes number of animals per group.

B: Intravenous treatment of subcutanenous tumors. Tumors were established in the hind flank of Balb/C mice by injecting 1×10^6 CT26 cells. When tumors reached approximately 10 mm^3, mice were treated every other day for 10 days (six doses total) with an intravenous injection of 5×10^8 pfu of the indicated virus. Control mice received six doses of 5×10^8 pfu equivalents of UV-inactivated AV2 VSV. Tumors were measured daily to calculate tumor volumes and animals were euthanized when tumors reached approximately 750 mm^3. Error bars denote SEM.

C: Mouse weights measured daily, for each treated group, for the 3 days before treatment to day 11 post-treatment. Error bars denote SEM.

D: Treatment of disseminated lung tumors. Lung tumors were established by injecting 3×10^5 CT26 cells into the tail vein of Balb/C mice. On day 12, mice were treated as follows: UVAV2 IV = 1 dose intravenously (5×10^8 pfu equivalents), AV2 IV = 1 dose AV2 intravenously (5×10^8 pfu), AV2 IN = 1 dose of AV2 intransally (5×10^7 pfu). Four days after treatment, all mice were sacrificed and their lungs were removed (hearts are visible for scale). Arrows indicate residual tumors. Inset: mice bearing CT-26 lung tumors were infected with AV3 GFP, and the lungs were removed and visualized as indicated.

E: Lung tumors were established as described above. On day 12, mice received 5×10^7 pfu of AV1 or AV2 by intranasal instillation every other day for 2 weeks (six doses total). "*n*" denotes number of mice in treatment group.

interferon-inducible cellular gene product Nup98. Indeed others have suggested that overexpression of Nup98 following interferon treatment may be sufficient to overcome an M-induced block of mRNA export. Interestingly, when we compared transcript levels in nuclear and cytoplasmic fractions following virus infection, we detected that nuclear export defects were more pronounced on some transcripts than others (D.F.S. and J.C.B., data not shown), which may reflect that the M-induced block may be specific for a subset of transcripts. It is interesting to note that in yeast, specific mRNA export factors (Yra1 and Mex67) have been shown to be responsible for the transport of different groups of transcripts (Hieronymus and Silver, 2003). Yra1 exports transcripts depending upon their rate of transcription whereas the Mex67 export protein does not discriminate on this basis (Hieronymus and Silver, 2003). Perhaps M protein in conjunction with Nup98 is targeting a specific set of proteins involved in the regulation of export of a subset of nuclear transcripts.

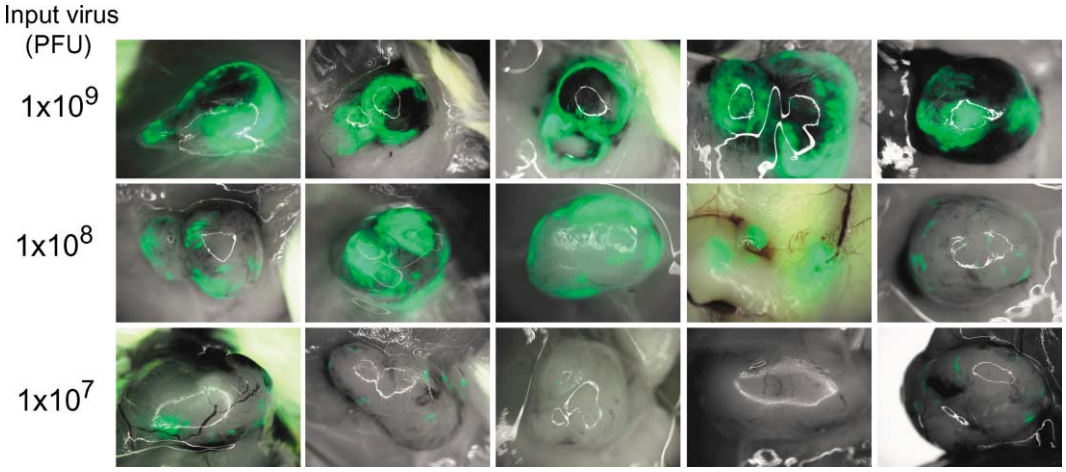

Figure 5. Threshold dose required for systemic delivery to subcutaneous tumors

Balb/C mice bearing CT26 subcutaneous tumors were treated with AV3 GFP intravenously at the indicated dose. At 24 hr, tumors were examined for fluorescence under a dissecting microscope. Tumors are shown in black and white, overlayed with fluorescent image.

It appears that host cell antiviral programs are initiated by activation of the latent transcription factors NFκB, c-JUN/ATF2, and IRF-3. Upon viral entry into the host cell, the transcription factors c-JUN and IRF-3 are phosphorylated by JNK and a recently identified virally activated kinase (Sharma et al., 2003), while NFκB is released from its inhibitor IkB through the action of upstream IKK(s) (DiDonato et al., 1997). The activated transcription factors translocate to the nucleus and coordinately form an enhancesome complex at the *IFN*-β promoter, leading to *IFN*-β induction (Wathelet et al., 1998). Here we refer to this as the primary transcriptional response to virus infection. We and others (Levy, 2002; Sato et al., 1998a) postulate that a secondary transcriptional wave (or positive feedback loop; Levy, 2002) is triggered by the IFN-β-dependent induction of a variety of interferon-stimulated genes. The data presented here with wild-type M protein help to delineate the distinction between these primary and secondary transcriptional events as well as identify several novel viral response genes (*GADD34*, *PUMA*). Following infection with viruses harboring mutant M proteins, it becomes clear that autocrine stimulation of the JAK/STAT signaling pathway by IFN-β leads to the production of secondary response genes like *IRF-7*, which in turn are critical for the tertiary induction of *IFN*-α genes (Morin et al., 2002). Indeed the M protein block of secondary and tertiary transcripts can be overcome by expressing a constitutively active version of IRF-7 (from a viral promoter) even in the presence of wild-type M protein. While our cell culture studies clearly delineate the role of VSV M in blunting the positive feedback loop that is dependent upon production of IFN-β and a functional interferon receptor, WT VSV infection still is capable of inducing interferon in intact animals (albeit more slowly and to lower levels). Others have shown that in virus-infected animals, an IFN-β-independent, systemic induction of interferon can occur in certain dendritic cell subsets; however, it is the local *IFN*-β-*dependent* production of interferon that is critical in determining the magnitude and ultimate success of an interferon-mediated antiviral response (Barchet et al., 2002). We show that the amount of interferon and the timing of its production in WT VSV-infected animals are not sufficient to protect against lethal infections. The results presented here and elsewhere (Barchet et al., 2002) are consistent with the idea that the rapid and robust local stimulation of interferon by AV strains in mice successfully attenuates virus replication in normal tissues (even of WT VSV, see Figure 1F). Our data indicates that defects in interferon signaling frequently occur during tumor evolution, with a majority of the cell lines in the NCI panel having an impaired response. Accumulating data have indicated that interferon is a multifunctional cytokine that can coordinately regulate cell growth, apoptosis, and antiviral pathways. Perhaps during tumor evolution, the selection for relentless growth and loss of apoptosis outstrips the occasional need for antiviral activity.

Kirn and colleagues argue that several factors are important in tumor killing by oncolytic virus therapeutics, including the effective delivery to multiple sites within the tumor, evasion of acquired and innate immunity, and rapid virus growth and spread (Wein et al., 2003). We have found that intravenous administration of VSV is an effective means of delivering virus to multiple sites within the tumor, and because of its broad tissue tropism and short replicative cycle, VSV can rapidly grow and spread within the tumor. These same traits, however, can be a lethal combination if virus growth in normal tissues is unchecked (Figures 1B and 1C). The attenuated viruses described here provide the best of both worlds; they grow rapidly in a broad spectrum of tumor cells but, because of their ability to trigger antiviral responses in normal cells, may be exceptionally safe to the treated animal.

One concern about the use of oncolytic virus therapeutics is the idea that a virulent strain could arise during virus propagation in a tumor. It is of interest to note, however, that it has proven impossible to date to select for VSV variants that are resistant to the antiviral effects of interferon (Novella et al., 1996), and we have shown that IFN-inducing mutants protect the host against infection with WT VSV (Figure 1F). Others have found that M mutations of the type described here cannot be complemented by mutations in other parts of M or other VSV genes (Coulon et al., 1990). In other words, only true revertants that

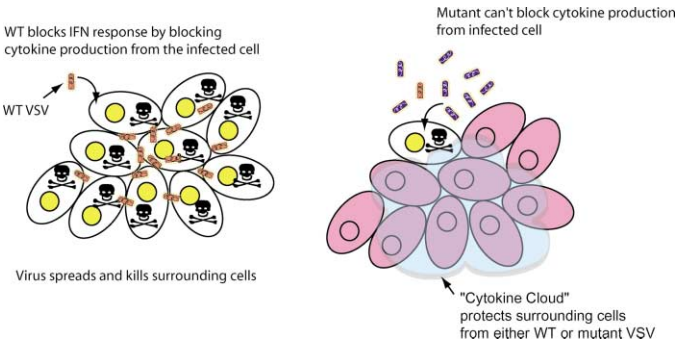

Figure 6. Model depicting how mutant VSV strains protect against virus spread

A: WT VSV blocks IFN production from infected cells. Uninfected cells are not protected from virus spread.

B: VSV strains defective in blocking nuclear/cytoplasmic mRNA export potently induce a "cytokine cloud" of antiviral cytokines (e.g., IFNs) protecting neighboring cells from virus spread.

convert arginine 51 back to methionine 51 can restore mutant M back to the wild-type phenotype. One of the viruses we have used in this work is a complete deletion of methionine 51, making the possibility of reversion to wild-type, even following several rounds of replication, remote. We speculate that in any population of interferon-responsive viruses where the majority of particles are potent inducers of interferon, it is unlikely that a wild-type variant could rise to dominance. The resulting "cytokine cloud" produced by infection with the IFN-inducing virus would protect the normal tissues of the host from the more virulent WT strain (Figure 6). Tumor killing would, however, be unaffected, as we have shown the majority of malignancies to be defective in responding to such a "cytokine cloud." We suggest that oncolytic viruses that trigger but do not disable antiviral responses will have a significantly improved therapeutic index over viruses that lack this property.

Experimental procedures

Viruses

The Indiana serotype of VSV was used throughout this study and was propagated in Vero cells. T1026R (Desforges et al., 2001) and TP3 (Desforges et al., 2001), herein referred to as AV1 and AV2, respectively, were shown in this study and elsewhere to be IFN-inducing mutants of the HR strain of wild-type VSV Indiana (Francoeur et al., 1987). WT GFP and AV3 GFP are recombinant viruses rescued from plasmids described below. The rescue procedure has been described in detail elsewhere (Lawson et al., 1995).

Constructs and viral rescue

Creation of the constitutively active IRF-7Δ (IRF-7Δ 247−467) has been previously described elsewhere (Lin et al., 2000). IRF-7Δ 247−467 was amplified by PCR using a forward primer to the Flag epitope with an additional 5′ VSV cap signal and an Xho1 linker (ATCGCTCGAGAACAGATGACTA CAAAGACGATGACGACAAG), together with a specific IRF-7 reverse primer containing a VSV poly A signal and an Nhe1 linker (ATCGGCTAGCAGTTTTT TTCAGGGATCCAGCTCTAGGTGG GCTGC). The PCR fragment was then cloned into the XhoI and NheI sites of the rVSV replicon vector pVSV-XN2 (provided by John Rose). Recovery of rVSV has been previously described (Lawson et al., 1995).

AV3 GFP is a recombinant virus with a deletion of methionine 51 in the M protein, as well as an extra cistron-encoding green fluorescent protein (GFP) inserted between the G and L sequences. Using T4 RNA ligase, an oligonucleotide containing a consensus T7 polymerase sequence was ligated to the single-stranded RNA genome of the HR strain of VSV. Reverse transcription coupled PCR was used to clone the entire genome as fragments into the pBluescript II SK+ vector (Stratgene). The PCR primers were designed in such a manner as to introduce unique restriction endonuclease sites between each of the five viral cistrons. Ligation of these fragments resulted in the construction of a full-length positive sense copy of the HR VSV genome with a T7 promoter sequence at the 5′ end of this anti-genome. Two overlapping oligonucleotides were synthesized to correspond to the hepatitis delta virus ribozyme sequence such that an XhoI site was introduced at the 3′ terminus of the ribozyme to facilitate further cloning. These oligos were annealed and extended using Klenow to form a blunt-ended double-stranded DNA fragment. A 300 bp fragment from the 3′ terminus of the anti-genome was PCR amplified and blunt end cloned to the ribozyme fragment. This fragment was subsequently cloned into the full-length genome construct described above via an internal AflII site in the 3′ terminus of the viral genome, and the XhoI site engineered into the ribozyme fragment. Finally, the T7 terminator sequence was cloned into this vector using the flanking XhoI and BssHII sites. This plasmid was designated pDSV1. To generate AV3VSV, we removed a XhoI/KpnI fragment spanning a region from within the P gene to within the G gene of pDSV1, replacing a similar fragment from within pXN, yielding the plasmid pXNDG. This facilitated the exchange of the M cistron from pXNDG, with one previously mutated by deleting the codon for methinonine at position 51 in the amino acid sequence using directed mutagenesis (Quickchange XL; Stratgene). Subsequently, the GFP coding sequence was removed from pEGFP (Clontech) by digesting with XhoI and XbaI and ligated into XhoI and NheI sites downstream of the additional stop/start sequence in the pXNDG vector.

WT GFP VSV was constructed by inserting the coding region of GFP from pEGFP (Clontech) between the XhoI and NheI sites in the pXN vector (provided by John Rose).

IFN ELISA

Interferon-α levels were measured using a Human Interferon-Alpha ELISA kit (PBL Biomedical) per manufacturer's directions. Various cell lines were infected with either WT VSV or AV1 or AV2 VSVs at an MOI of 10. One hundred microliters of culture medium was collected at 48 hr post-infection and incubated in a 96-well microtiter plate along with standards supplied by manufacturer. IFN-β production was measured at 10 hr post-infection using a human IFN-β detection kit (TFB INC; Tokyo, Japan). Samples were processed as per manufacturer's instructions and then read on a DYNEX plate reader at primary wavelength of 450 nm with a reference wavelength of 630 nm.

A variation of the above assay was used to determine the impact of IFN-β on IFN-α production. Briefly, 24-well plates of OVCAR-4 cells were either mock infected or infected with WT GFP VSV or AV3 GFP VSV at an MOI of 5 for 30 min. These wells were then washed with PBS and fed with OptiMEM (Invitrogen) or OptiMEM supplemented with various concentrations of antibody as indicated. To neutralize IFN-β in the media, an anti-IFN-β antibody was used (AHC4024; Biosource International), and as a nonspecific control, an anti-HA antibody was used (sc-805; Santa Cruz). Twenty-two hours post-infection, 100 μl of media from each well was assayed for IFN-α production using a Human IFN-α ELISA (PBL Biomedical) kit as described.

Mouse serum IFN-α levels were assayed using a mouse Interferon-Alpha ELISA kit (PBL Biomedical). Balb/C females (10 weeks old; Charles River) were injected intravenously with either PBS or 1×10^8 pfu of WT GFP or AV3 GFP diluted in PBS. At the indicated times post-infection, blood was collected from the saphenous vein of each mouse into heparinized tubes and centrifuged to obtain serum. For each sample, 5 μl of serum was diluted in 95 μl of PBS and assayed as per manufacturer's instructions.

Determination of in vivo toxicity of VSV mutant viruses

Eight- to ten-week-old female mice (strains as indicated; Charles River) were divided into groups of five and infected with dilutions of virus from 1×10^{10} pfu to 1×10^2 pfu by the indicated route. Animals were monitored for weight loss, dehydration, piloerection, huddling behavior, respiratory distress, and hind limb paralysis. Mice showing moderate to severe morbidity were euthanized as per good laboratory practices prescribed by the CCAS. Lethal dose 50 values were calculated by the Karber-Spearman method.

Four-week-old Balb/C mice or Balb/C interferon-α receptor knockout

mice (IFNAR$^{-/-}$) (Steinhoff et al., 1995) were infected intranasally with 10^4 pfu of either WT VSV, AV1, or AV2. Mice were monitored for signs of morbidity and were euthanized upon signs of severe respiratory distress.

Determination of in vivo toxicity of mixed samples of WT and mutant VSV strains

Groups of three mice were infected by intranasal instillation with either WT, AV2, or mixtures of these strains as indicated. Mice were monitored for signs of morbidity and were euthanized upon signs of severe respiratory distress or hind limb paralysis.

MTS assay

In each experiment, the test cell line was seeded into 96-well plates at 3×10^4 cells/well in growth medium (DMEM-F12-HAM + 10% FBS; Invitrogen). Following overnight incubation (37°C, 5% CO_2), media were removed by aspiration and to each well was added 20 μl of virus-containing media (α-MEM, no serum) ranging in 10-fold increments from 3×10^6 pfu/well to 3 pfu/well or negative control media containing no virus. Each virus dose tested was done in replicates of six. After a 60 min incubation to allow virus attachment, 80 μl of growth medium was added to each well, and the plates were incubated for another 48 hr. Cell viability was measured using the CellTitre 96 AQ_{ueous} MTS reagent (Promega).

To assay for IFN defects, cell lines were pretreated with either 5 units/ml of IFN-α (Schering) or IFN-β (PBL Biomedical) for 12 hr and then challenged with a range of doses of WT VSV as described above. A standard MTS assay was performed and the results compared from nonpretreated cells.

Microarray

OVCAR4 cells either mock treated or infected with WT and AV strains were harvested in PBS, pelleted, and resuspended in 250 μl of resuspension buffer (10 mM Tris [pH 7.4], 15 mM NaCl, 12.5 mM $MgCl_2$). Six hundred microliters of Lysis buffer (25 mM Tris [pH 7.4], 15 mM Nacl, 12.5 mM $MgCl_2$ 5% sucrose, and 1% NP-40) was added and the lysates were incubated at 4°C for 10 min with occasional vortexing. Nuclei were collected by centrifugation at 1000 × g for 3 min. The supernatant (cytoplasmic fraction) was collected and frozen at −80°C while the pellet (nuclear fraction) was washed once with 250 μl of lysis buffer and frozen. Total RNA was isolated from both nuclear and cytoplasmic fractions using the Qiagen RNeasy kit (as per manufacturer's instructions; Qiagen) followed by LiCl precipitation to concentrate each sample. Twenty micrograms of each RNA sample was processed according to manufacturer's standard protocol (Affymetrix) and hybridized to an Affymetrix HGA133u A chip. Each chip was scaled to 1500, normalized to the 100 normalization control genes present on each chip, then all nuclear samples were normalized to the mock nuclear sample on a per gene basis, while the cytoplasmic fractions were normalized to the corresponding mock cytoplasmic sample. Data were analyzed using Genespring software (SiliconGenetics).

Western blotting

OVCAR4 cells were grown in RPMI (Wisent) supplemented with 10% fetal bovine serum (Wisent). 1×10^7 cells were plated in 10 cm dishes the day prior to infection. For infection, the media were removed and replaced with RPMI alone prior to the addition of 5×10^7 pfu per VSV viral strain. One hour after virus addition, media were removed and replaced with RPMI supplemented with 10% FBS for the remaining duration of the experiment. Cells were lysed in standard NP-40 lysis buffer, and 75 μg of whole-cell extract was run on SDS-polyacrylamide gel and blotted with the following antibodies as indicated: IRF-7 (sc-9083; Santa Cruz), IRF-3 (sc-9082; Santa Cruz), ISG56 (a gift from Ganes Sen), VSV-N (polyclonal directed against the full-length Indiana N protein), and Actin (sc-8432; Santa Cruz).

Quantitative PCR of Interferon-β mRNA

Nuclear and cytoplasmic total RNA from infected or mock-infected OVCAR4 cells was isolated as per manufacturer's instruction (RNeasy; Qiagen). Four micrograms of total RNA was DNase treated and reverse transcribed. Quantitative PCR was performed in triplicate to amplify IFN-β and HPRT targets from each using Roche Lightcycler technology (Roche Diagnostics). Crossing points were converted to absolute quantities based on standard curves generated for each target amplicon. IFN-β signal was subsequently normalized to HPRT as HPRT levels are unchanged during the course of these infections (data not shown). Primers used to amplify IFN-β were sense 5′-TTGTGCTTCTCCACTACAGC-3′; antisense 5′-CTGTAAGTCTGTTAATGAAG-3′ and HPRT primers were sense 5′-TGACACTGGCAAAACAATGCA-3′, antisense 5′-GGTCCTTTTCACCAGCAAGCT-3′.

RT-PCR of interferon-α and interferon-stimulated genes

A549 cells cultured in F12K medium supplemented with 10% FBS were infected with WT or AV strains (MOI 10). RNA was extracted 4 hr post-infection using Trizol (Invitrogen) according to the manufacturer's instructions. One microgram of RNA was reverse transcribed with Oligo dT primers and 5% of RT was used as template in a Taq PCR. Primers used were as follows: Mx forward primer 5′-TTTGTTGTTTCCGAAGTGGAC-3′ and reverse primer 5′-TTTCTTCAGTTTCAGCACCAG-3′; VSV N forward primer 5′-ATGTCTGTTACAGTCAAGAGAATC-3′ and reverse primer 5′-TCATTTGTCAAATTCTGACTTAGCATA-3′; RANTES forward primer 5′-TACACCAGTGGCAAGTGCTCCAACCCAG-3′ and reverse primer 5′-GTCTCGAACTCCTGACCTCAAGTGATCC-3′; β-actin forward primer 5′-ACAATGAGCTGCTGGTGGCT-3′ and reverse primer 5′-GATGGGCACAGTGTGGGTGA-3′.

Ovarian xenograft cancer model in athymic mice

Approximately 1×10^6 ES-2 human ovarian carcinoma cells were injected into the peritoneal cavity of CD-1 athymic mice (Charles River). Ascites development is generally observed by day 15 after cell injection. On days 12, 14, and 16, mice were treated with 1×10^9 AV2 virus or 1×10^9 pfu equivalent of UV-inactivated AV2 VSV by intraperitoneal injection. Mice were monitored for morbidity and euthanized upon development of ascites.

Subcutaneous tumor model

To establish subcutaneous tumors, 8- to 10-week-old Balb/C female mice (Charles River) were shaved on the right flank and injected with 1×10^6 CT26 colon carcinoma cells (Kashtan et al., 1992) syngeneic for Balb/C mice. These tumors were allowed to develop until they reached approximately 10 mm^3, at which time virus treatments were initiated. Groups of animals received 1 of 6 doses of the indicated virus every other day for 2 weeks. Each dose of 5×10^8 pfu was administered by tail vein infection. Tumors were measured daily and volumes calculated using the formula 1/2(L*W*H). Mice were weighed daily and monitored for weight loss, dehydration, piloerection, huddling behavior, respiratory distress, and hind limb paralysis. Animals were euthanized when their tumor burden reached end point (750 mm^3).

Lung model

Lung tumors were established in 8- to 10-week-old female Balb/C mice (Charles River) by tail vein injection of 3×10^5 CT26 cells (Specht et al., 1997). On days 10, 12, 14, 17, 19, and 21, groups of mice received 5×10^7 pfu of the indicated virus by intranasal instillation as described elsewhere (Stojdl et al., 2000a). Mice were weighed daily and monitored for weight loss, dehydration, piloerection, huddling behavior, respiratory distress, and hind limb paralysis. Animals were euthanized at the onset of respiratory distress and their lungs examined to confirm tumor development.

Visualization of GFP-expressing VSV strains in vivo

Female Balb/c mice (Charles River) were injected with 3×10^5 CT26 cells via the vein to initiate pulmonary metastases. On day 17, mice were injected intravenously with 2.5×10^8 pfu AV3 GFP VSV. Hind limb tumors were seeded by subcutaneous injection with 3×10^5 CT26 cells. When tumors reached a volume of approximately 400 mm^3, mice were injected intravenously with 2.5×10^8 pfu of AV3 GFP VSV. At the indicated times, mice were euthanized and tumors examined using a Leica MZFLIII microscope with a standard GFP filter set. Pictures were captured with a Nikon Coolpix 100 camera. Overlayed images were generated using Adobe Photoshop 7.0.

Acknowledgments

B.D.L. is a recipient of a fellowship from the National Cancer Institute of Canada (NCIC). This work was funded by grants from the NCIC and the Canadian Institutes of Health Research awarded to J.C.B. Funding for portions of this work was also provided by Wellstat Biologics Corporation. J.C.B. is Senior Scientist of Cancer Care Ontario. We thank John Rose for plasmids required to produce recombinant VSVs and Ken Garson for critical reading of the manuscript.

Received: April 15, 2003
Revised: July 31, 2003
Published: October 20, 2003

References

Ahmed, M., McKenzie, M.O., Puckett, S., Hojnacki, M., Poliquin, L., and Lyles, D.S. (2003). Ability of the matrix protein of vesicular stomatitis virus to suppress beta interferon gene expression is genetically correlated with the inhibition of host RNA and protein synthesis. J. Virol. *77*, 4646–4657.

Balachandran, S., and Barber, G.N. (2000). Vesicular stomatitis virus (VSV) therapy of tumors. IUBMB Life *50*, 135–138.

Balachandran, S., Roberts, P.C., Brown, L.E., Truong, H., Pattnaik, A.K., Archer, D.R., and Barber, G.N. (2000). Essential role for the dsRNA-dependent protein kinase PKR in innate immunity to viral infection. Immunity *13*, 129–141.

Barchet, W., Cella, M., Odermatt, B., Asselin-Paturel, C., Colonna, M., and Kalinke, U. (2002). Virus-induced interferon alpha production by a dendritic cell subset in the absence of feedback signaling in vivo. J. Exp. Med. *195*, 507–516.

Bell, J.C., Garson, K.A., Lichty, B.D., and Stojdl, D.F. (2002). Oncolytic viruses: programmable tumour hunters. Curr. Gene Ther. *2*, 243–254.

Bello, M.J., de Campos, J.M., Kusak, M.E., Vaquero, J., Sarasa, J.L., Pestana, A., and Rey, J.A. (1994). Molecular analysis of genomic abnormalities in human gliomas. Cancer Genet. Cytogenet. *73*, 122–129.

Blondel, D., Harmison, G.G., and Schubert, M. (1990). Role of matrix protein in cytopathogenesis of vesicular stomatitis virus. J. Virol. *64*, 1716–1725.

Coulon, P., Deutsch, V., Lafay, F., Martinet-Edelist, C., Wyers, F., Herman, R.C., and Flamand, A. (1990). Genetic evidence for multiple functions of the matrix protein of vesicular stomatitis virus. J. Gen. Virol. *71*, 991–996.

Desforges, M., Charron, J., Berard, S., Beausoleil, S., Stojdl, D.F., Despars, G., Laverdiere, B., Bell, J.C., Talbot, P.J., Stanners, C.P., and Poliquin, L. (2001). Different host-cell shutoff strategies related to the matrix protein lead to persistence of vesicular stomatitis virus mutants on fibroblast cells. Virus Res. *76*, 87–102.

DiDonato, J.A., Hayakawa, M., Rothwarf, D.M., Zandi, E., and Karin, M. (1997). A cytokine-responsive IkappaB kinase that activates the transcription factor NF-kappaB. Nature *388*, 548–554.

Ferran, M.C., and Lucas-Lenard, J.M. (1997). The vesicular stomatitis virus matrix protein inhibits transcription from the human beta interferon promoter. J. Virol. *71*, 371–377.

Francoeur, A.M., Poliquin, L., and Stanners, C.P. (1987). The isolation of interferon-inducing mutants of vesicular stomatitis virus with altered viral P function for the inhibition of total protein synthesis. Virology *160*, 236–245.

Genin, P., Algarte, M., Roof, P., Lin, R., and Hiscott, J. (2000). Regulation of RANTES chemokine gene expression requires cooperativity between NF-kappa B and IFN-regulatory factor transcription factors. J. Immunol. *164*, 5352–5361.

Gromeier, M., and Wimmer, E. (2001). Viruses for the treatment of malignant glioma. Curr. Opin. Mol. Ther. *3*, 503–508.

Hawkins, L.K., Lemoine, N.R., and Kirn, D. (2002). Oncolytic biotherapy: a novel therapeutic plafform. Lancet Oncol. *3*, 17–26.

Her, L.S., Lund, E., and Dahlberg, J.E. (1997). Inhibition of Ran guanosine triphosphatase-dependent nuclear transport by the matrix protein of vesicular stomatitis virus. Science *276*, 1845–1848.

Hieronymus, H., and Silver, P.A. (2003). Genome-wide analysis of RNA-protein interactions illustrates specificity of the mRNA export machinery. Nat. Genet. *33*, 155–161.

Huneycutt, B.S., Bi, Z., Aoki, C.J., and Reiss, C.S. (1993). Central neuropathogenesis of vesicular stomatitis virus infection of immunodeficient mice. J. Virol. *67*, 6698–6706.

Ikeda, K., Wakimoto, H., Ichikawa, T., Jhung, S., Hochberg, F.H., Louis, D.N., and Chiocca, E.A. (2000). Complement depletion facilitates the infection of multiple brain tumors by an intravascular, replication-conditional herpes simplex virus mutant. J. Virol. *74*, 4765–4775.

Jayakar, H.R., Murti, K.G., and Whitt, M.A. (2000). Mutations in the PPPY motif of vesicular stomatitis virus matrix protein reduce virus budding by inhibiting a late step in virion release. J. Virol. *74*, 9818–9827.

Kashtan, H., Rabau, M., Mullen, J.B., Wong, A.H., Roder, J.C., Shpitz, B., Stern, H.S., and Gallinger, S. (1992). Intra-rectal injection of tumour cells: a novel animal model of rectal cancer. Surg. Oncol. *1*, 251–256.

Kruyt, F.A., and Curiel, D.T. (2002). Toward a new generation of conditionally replicating adenoviruses: pairing tumor selectivity with maximal oncolysis. Hum. Gene Ther. *13*, 485–495.

Lawson, N.D., Stillman, E.A., Whitt, M.A., and Rose, J.K. (1995). Recombinant vesicular stomatitis viruses from DNA. Proc. Natl. Acad. Sci. USA *92*, 4477–4481.

Levy, D.E. (2002). Whence interferon? Variety in the production of interferon in response to viral infection. J. Exp. Med. *195*, F15–F18.

Lin, R., Mamane, Y., and Hiscott, J. (2000). Multiple regulatory domains control IRF-7 activity in response to virus infection. J. Biol. Chem. *275*, 34320–34327.

Linge, C., Gewert, D., Rossmann, C., Bishop, J.A., and Crowe, J.S. (1995). Interferon system defects in human malignant melanoma. Cancer Res. *55*, 4099–4104.

Lu, R., Au, W.C., Yeow, W.S., Hageman, N., and Pitha, P.M. (2000). Regulation of the promoter activity of interferon regulatory factor-7 gene. Activation by interferon and silencing by hypermethylation. J. Biol. Chem. *275*, 31805–31812.

Lyles, D.S., McKenzie, M.O., Ahmed, M., and Woolwine, S.C. (1996). Potency of wild-type and temperature-sensitive vesicular stomatitis virus matrix protein in the inhibition of host-directed gene expression. Virology *225*, 172–180.

Matin, S.F., Rackley, R.R., Sadhukhan, P.C., Kim, M.S., Novick, A.C., and Bandyopadhyay, S.K. (2001). Impaired alpha-interferon signaling in transitional cell carcinoma: lack of p48 expression in 5637 cells. Cancer Res. *61*, 2261–2266.

Morin, P., Braganca, J., Bandu, M.T., Lin, R., Hiscott, J., Doly, J., and Civas, A. (2002). Preferential binding sites for interferon regulatory factors 3 and 7 involved in interferon-A gene transcription. J. Mol. Biol. *316*, 1009–1022.

Nakaya, T., Sato, M., Hata, N., Asagiri, M., Suemori, H., Noguchi, S., Tanaka, N., and Taniguchi, T. (2001). Gene induction pathways mediated by distinct IRFs during viral infection. Biochem. Biophys. Res. Commun. *283*, 1150–1156.

Newcomb, W.W., Tobin, G.J., McGowan, J.J., and Brown, J.C. (1982). In vitro reassembly of vesicular stomatitis virus skeletons. J. Virol. *41*, 1055–1062.

Norman, K.L., Farassati, F., and Lee, P.W. (2001). Oncolytic viruses and cancer therapy. Cytokine Growth Factor Rev. *12*, 271–282.

Novella, I.S., Cilnis, M., Elena, S.F., Kohn, J., Moya, A., Domingo, E., and Holland, J.J. (1996). Large-population passages of vesicular stomatitis virus in interferon-treated cells select variants of only limited resistance. J. Virol. *70*, 6414–6417.

Petersen, J.M., Her, L.S., Varvel, V., Lund, E., and Dahlberg, J.E. (2000). The matrix protein of vesicular stomatitis virus inhibits nucleocytoplasmic transport when it is in the nucleus and associated with nuclear pore complexes. Mol. Cell. Biol. *20*, 8590–8601.

Sato, M., Hata, N., Asagiri, M., Nakaya, T., Taniguchi, T., and Tanaka, N. (1998a). Positive feedback regulation of type I IFN genes by the IFN-inducible transcription factor IRF-7. FEBS Lett. *441*, 106–110.

Sato, M., Tanaka, N., Hata, N., Oda, E., and Taniguchi, T. (1998b). Involvement of the IRF family transcription factor IRF-3 in virus-induced activation of the IFN-beta gene. FEBS Lett. *425*, 112–116.

Sharma, S., tenOever, B.R., Grandvaux, N., Zhou, G.P., Lin, R., and Hiscott, J. (2003). Triggering the interferon antiviral response through an IKK-related pathway. Science *300*, 1148–1151.

Specht, J.M., Wang, G., Do, M.T., Lam, J.S., Royal, R.E., Reeves, M.E., Rosenberg, S.A., and Hwu, P. (1997). Dendritic cells retrovirally transduced with a model antigen gene are therapeutically effective against established pulmonary metastases. J. Exp. Med. *186*, 1213–1221.

Steinhoff, U., Muller, U., Schertler, A., Hengartner, H., Aguet, M., and Zinkernagel, R.M. (1995). Antiviral protection by vesicular stomatitis virus-specific antibodies in alpha/beta interferon receptor-deficient mice. J. Virol. *69*, 2153–2158.

Stojdl, D.F., Abraham, N., Knowles, S., Marius, R., Brasey, A., Lichty, B.D., Brown, E.G., Sonenberg, N., and Bell, J.C. (2000a). The murine double-stranded RNA-dependent protein kinase PKR is required for resistance to vesicular stomatitis virus. J. Virol. *74*, 9580–9585.

Stojdl, D.F., Lichty, B., Knowles, S., Marius, R., Atkins, H., Sonenberg, N., and Bell, J.C. (2000b). Exploiting tumor-specific defects in the interferon pathway with a previously unknown oncolytic virus. Nat. Med. *6*, 821–825.

Sun, W.H., Pabon, C., Alsayed, Y., Huang, P.P., Jandeska, S., Uddin, S., Platanias, L.C., and Rosen, S.T. (1998). Interferon-alpha resistance in a cutaneous T-cell lymphoma cell line is associated with lack of STAT1 expression. Blood *91*, 570–576.

Terstegen, L., Gatsios, P., Ludwig, S., Pleschka, S., Jahnen-Dechent, W., Heinrich, P.C., and Graeve, L. (2001). The vesicular stomatitis virus matrix protein inhibits glycoprotein 130-dependent STAT activation. J. Immunol. *167*, 5209–5216.

von Kobbe, C., van Deursen, J.M., Rodrigues, J.P., Sitterlin, D., Bachi, A., Wu, X., Wilm, M., Carmo-Fonseca, M., and Izaurralde, E. (2000). Vesicular stomatitis virus matrix protein inhibits host cell gene expression by targeting the nucleoporin Nup98. Mol. Cell *6*, 1243–1252.

Wakimoto, H., Ikeda, K., Abe, T., Ichikawa, T., Hochberg, F.H., Ezekowitz, R.A., Pasternack, M.S., and Chiocca, E.A. (2002). The complement response against an oncolytic virus is species-specific in its activation pathways. Mol. Ther. *5*, 275–282.

Wakimoto, H., Johnson, P.R., Knipe, D.M., and Chiocca, E.A. (2003). Effects of innate immunity on herpes simplex virus and its ability to kill tumor cells. Gene Ther. *10*, 983–990.

Wathelet, M.G., Lin, C.H., Parekh, B.S., Ronco, L.V., Howley, P.M., and Maniatis, T. (1998). Virus infection induces the assembly of coordinately activated transcription factors on the IFN-beta enhancer in vivo. Mol. Cell *1*, 507–518.

Wein, L.M., Wu, J.T., and Kirn, D.H. (2003). Validation and analysis of a mathematical model of a replication-competent oncolytic virus for cancer treatment: implications for virus design and delivery. Cancer Res. *63*, 1317–1324.

Wong, L.H., Krauer, K.G., Hatzinisiriou, I., Estcourt, M.J., Hersey, P., Tam, N.D., Edmondson, S., Devenish, R.J., and Ralph, S.J. (1997). Interferon-resistant human melanoma cells are deficient in ISGF3 components, STAT1, STAT2, and p48-ISGF3gamma. J. Biol. Chem. *272*, 28779–28785.

Yoon, S.K., Armentano, D., Wands, J.R., and Mohr, L. (2001). Adenovirus-mediated gene transfer to orthotopic hepatocellular carcinomas in athymic nude mice. Cancer Gene Ther. *8*, 573–579.

Yuan, H., Puckett, S., and Lyles, D.S. (2001). Inhibition of host transcription by vesicular stomatitis virus involves a novel mechanism that is independent of phosphorylation of TATA-binding protein (TBP) or association of TBP with TBP-associated factor subunits. J. Virol. *75*, 4453–4458.